available at www.sciencedirect.com

ScienceDirect

www.elsevier.com/locate/brainres

BRAIN RESEARCH

Research Report

Layer specific changes of astroglial gap junctions in the rat cerebellar cortex by persistent Borna Disease Virus infection

*Christiane Köster-Patzlaff, Seyed Mehdi Hosseini, Bernhard Reuss**

Center for Anatomy, Neuroanatomy, University of Göttingen, Kreuzbergring 36, 37075 Göttingen, Germany

ARTICLE INFO

Article history:
Accepted 11 April 2008
Available online 30 April 2008

Keywords:
Astroglia
Gap junction
Connexin
Borna Disease Virus
Cerebellum

ABSTRACT

Neonatal Borna Disease Virus (BDV) infection of the Lewis rat brain, leads to Purkinje cell degeneration, in association with astroglial activation. Since astroglial gap junctions (GJ) are known to influence neuronal degeneration, we investigated BDV dependent changes in astroglial GJ connexins (Cx) Cx43, and Cx30 in the Lewis rat cerebellum, 4, and 8 weeks after neonatal infection. On the mRNA level, RT-PCR demonstrated a BDV dependent increase in cerebellar Cx43, and a decrease in Cx30, 8, but not 4 weeks p.i. On the protein level, Western blot analysis revealed no overall upregulation of Cx43, but an increase of its phosphorylated forms, 8 weeks p.i. Cx30 protein was downregulated. Immunohistochemistry revealed a BDV dependent reduction of Cx43 in the granular layer (GL), 4 weeks p.i. 8 weeks p.i., Cx43 immunoreactivity recovered in the GL, and was induced in the molecular layer (ML). Cx30 revealed a BDV dependent decrease in the GL, both 4, and 8 weeks p.i. Changes in astroglial Cxs correlated not with expression of the astrogliotic marker GFAP, which was upregulated in radial glia. With regard to functional coupling, primary cerebellar astroglial cultures, revealed a BDV dependent increase of Cx43, and Cx30 immunoreactivity and in spreading of the GJ permeant dye Lucifer Yellow. These results demonstrate a massive, BDV dependent reorganization of astroglial Cx expression, and of functional GJ coupling in the cerebellar cortex, which might be of importance for the BDV dependent neurodegeneration in this brain region.

© 2008 Elsevier B.V. All rights reserved.

1. Introduction

Neonatal infection of the Lewis rat brain with the Borna Disease Virus (BDV), is a model system to study the consequences of persistent viral infections for brain function, morphology, and behaviour (Pletnikov et al. 2001, 2002; Lancaster et al., 2006; for a review see Hornig et al. (2003)). Amongst others, neonatal BDV infections cause a loss of Purkinje neurons, and induce sensorimotor deficits, characteristic for impaired cerebellar functions (Bautista et al., 1994; Eisenman et al., 1999; Pletnikov et al., 2001). Although some of the neuronal aspects of BDV dependent Purkinje cell death, such as reduced levels of neurotrophin receptors, and increased rates of apoptotic cell death, are well characterized (Zocher et al., 2000), the role of astroglial changes is far from being clear.

In the healthy brain, astrocytes are important for the maintenance of CNS homeostasis (Schousboe and Waagepetersen, 2005), and for long range calcium signalling (Scemes et al., 1998; Schipke et al., 2002). Since synapses are often enwrapped by astrocytic processes, astrocytes are thought to modulate synaptic transmission (Ventura and Harris, 1999). Also cerebellar Purkinje neurons are ensheathed by astroglial endfeet, which

* *Corresponding author.*
E-mail address: breuss@gwdg.de (B. Reuss).

Abbreviations: BDV, Borna Disease Virus; BDV-p40, BDV Nucleoprotein 40; Cx, connexin; GFAP, glial fibrillar acidic protein; GJ, gap junction; GL, granular layer; LY, Lucifer Yellow; ML, molecular layer; p.i., post infection

0006-8993/$ – see front matter © 2008 Elsevier B.V. All rights reserved.
doi:10.1016/j.brainres.2008.04.062

probably modulate synaptic activity, and wiring (Meshul et al., 1987), as well as electrophysiological characteristics of the cerebellar cortex (Drake-Baumann and Seil, 1999). By previous reports, markers of reactive astrogliosis, like vimentin, and GFAP, have been demonstrated to be induced by persistent BDV infection (Carbone et al., 1989, 1991), suggesting a role of astrocytes during BDV dependent neuron degeneration.

Astrocytes are coupled by gap junctions (GJ), and GJ coupling is known to affect most astroglial functions (Charles et al., 1992; Farahani et al., 2005; Froes and de Carvalho, 1998; Naus and Bani-Yaghoub, 1998; Naus et al., 1999; Rozental et al., 2000a; Spray et al., 1999; Stout et al., 2002; Tabernero et al., 2006; Ye et al., 2003). GJs mediate the direct cytoplasmic contact between adjacent astrocytes, thereby integrating them into a functional syncytium. Within this syncytium, neurotransmitters, metabolites, waste products, and ions are exchanged, resulting in spatial buffering of local concentration changes of these substances (Froes and de Carvalho, 1998; Spray et al., 1999).

GJs are formed by connexins (Cx), a protein family with more than 20 members, which are classified by their theoretical molecular weight (see Söhl and Willecke (2003) for a review). Therefore the molecular weight of the predominant astroglial Cx subtype Cx43, is around 43 kDa, whereas that of Cx30, another astroglial Cx, is around 30 kDa (Altevogt and Paul, 2004; Dermietzel et al., 2000; Nagy et al., 2001, 2003). Also cerebellar astrocytes are known to express cx43 (Micevych and Abelson, 1991; Belliveau and Naus 1995), whereas only limited information exists on Cx30 in that brain region (Condorelli et al., 2002). However, in other brain regions, Cx30 is preferentially localized in astrocytes (Nagy et al., 1999). Despite its astroglial expression, during kainate-induced seizures in the rat brain, Cx30 mRNA levels are also induced in neuronal

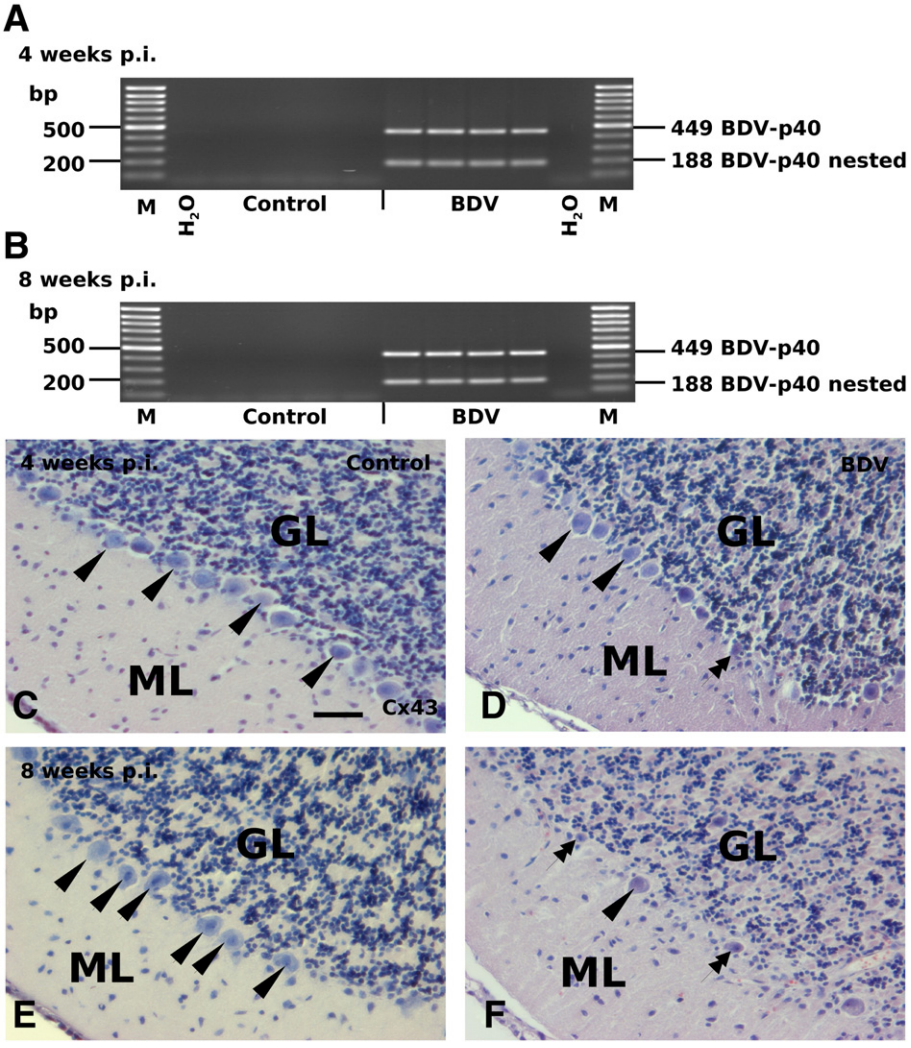

Fig. 1 – Confirmation of successful BDV infection in the brain samples investigated, by standard, and nested RT-PCR, and by histological analysis. (A) Fluorescence image of an ethidium bromide stained agarose gel, demonstrating BDV-p40 specific reaction products 4 weeks p.i., to be obtained only from RNA samples of BDV-infected, but not of control treated animals. (B) Also 8 weeks p.i., BDV-p40 specific PCR bands are obtained exclusively from brain samples of BDV-infected animals. (C–F) Morphological differences between the cerebellar cortex of non-infected (C, E), and BDV-infected (D, F) Lewis rats, 4 (C, D), and 8 (E, F) weeks p.i. 4 weeks p.i., in BDV-infected rats, a reduction of Purkinje neurons can be observed, whereas 8 weeks p.i., Purkinje neurons are almost completely lost. Bar = 100 μm; bp = base pairs; GL = granular layer; ML = molecular layer; Arrowhead = intact Purkinje neurons; double Arrow = degenerating Purkinje neurons. M = 100 bp marker; p.i. = post infection.

cells, undergoing apoptotic cell death (Condorelli et al., 2002), a feature that might be also of importance for the present study.

A special type of astrocyte-like radial glia in the cerebellar cortex are Bergmann glia cells, cell bodies of which are found adjacent to Purkinje cells. They extend long radial processes into the molecular layer (ML) of the cerebellar cortex, where they ensheathe the synapses formed between parallel fibers, and Purkinje cell dendrites. Although Bergmann glia are known to be electrically coupled by GJs (Müller et al., 1996), Cx types expressed in these cells have not yet been clarified except for Cx29 in mice (Eiberger et al., 2006).

From previous studies by other groups, several infectious agents like protozoans, and bacteria, have been demonstrated to change astroglial coupling, and Cx expression (Campos de Carvalho et al., 1998; Esen et al., 2007). However, although astrocytes are primary sites of BDV replication (Carbone et al., 1989, 1991), and BDV is known to modulate astroglial functioning (Billaud et al., 2000), effects of persistent viral infections, on astroglial GJs have been reported only very recently (Köster-Patzlaff et al., 2007; Fatemi et al., 2008; Eugenin and Berman, 2007). In a previous study, we have analyzed BDV dependent changes in astroglial Cx expression in the hippocampal formation, another brain region being affected by persistent BDV infections (Köster-Patzlaff et al., 2007). In the present study, we analyze the expression of Cx43 and Cx30, as well as the astrogliotic marker GFAP during BDV dependent Purkinje cell degeneration *in vivo*, and of BDV dependent changes in functional GJ coupling in primary cerebellar astroglial cultures *in vitro*.

2. Results

2.1. *Verification of BDV infections by RT-PCR and morphological effects*

Persistent BDV infection of the brain samples used here, was verified by amplification of cDNA fragments, specific for the BDV nucleoprotein BDV-p40, by a standard, and a nested RT-PCR protocol (Figs. 1A and B). Both, 4, and 8 weeks p.i., BDV-p40

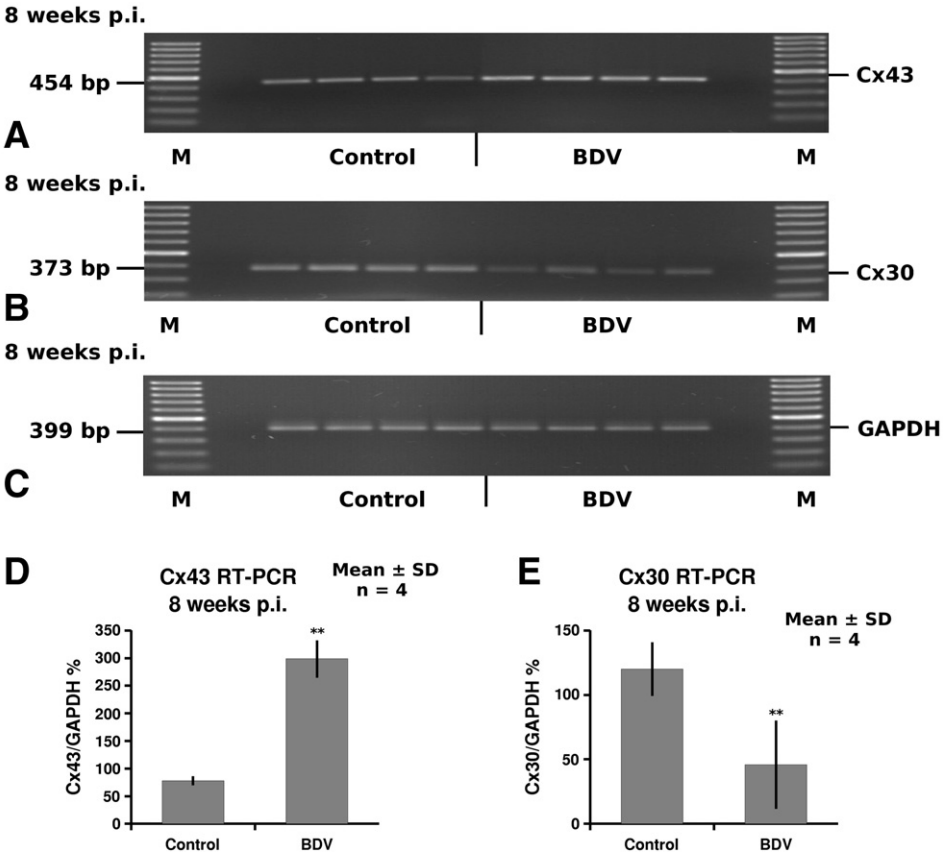

Fig. 2 – Expression of Cx43 and Cx30 mRNAs in the cerebellar cortex of BDV-infected, and non-infected Lewis rats, 8 weeks p.i., as revealed by RT-PCR. (A) Ethidium bromide stained agarose gel of an RT-PCR, for the detection of Cx43 in total RNA of the cerebellar cortex, from non-infected control animals, and BDV-infected rats, 8 weeks p.i. (B) Ethidium bromide stained agarose gel of an RT-PCR, for the detection of Cx30, in total RNA of the cerebellar cortex, from non-infected control animals, and BDV-infected rats, 8 weeks p.i. (C) Ethidium bromide stained agarose gel, of an RT-PCR for the detection of GAPDH in total RNA, from the cerebellar cortex, of non-infected control animals, and BDV-infected rats, 8 weeks p.i. (D) Graph of the statistical evaluation, of the intensity of Cx43 specific PCR bands, shown in (A), compared to the corresponding bands of GAPDH, as shown in (C). (E) Graph of the statistical analysis, of the densitometric evaluation of Cx30 specific PCR bands, shown in (B), compared to the corresponding bands of GAPDH, as shown in (C). Whereas the mRNA expression of Cx43 is significantly increased, mRNA of Cx30 shows a BDV dependent decrease, 8 weeks p.i. Error bars = standard deviation, $^{**}p \leq 0.01$.

amplification products could be detected by standard, and nested RT-PCR in RNA samples of BDV-infected brains, but not of non-infected controls. In addition, morphological analysis of hematoxylin/eosin stained histological sections (Figs. 1C–F), demonstrated a decrease in numbers of Purkinje cells in neonatally BDV-infected Lewis rats (Figs. 1D, F), as compared to non-infected controls (Figs. 1C, E), which was most prominent 8 weeks p.i. (Fig. 1F).

2.2. *BDV dependent changes in expression of Cx43 and Cx30 as revealed by RT-PCR*

As shown by RT-PCR using total RNA of the cerebellar cortex from BDV-infected, and non-infected rats, 8 weeks p.i. (Fig. 2A), Cx43 mRNA was induced in RNA samples of BDV-infected rats, as compared to those from non-infected controls. In contrast to that, mRNA expression of Cx30 was reduced by BDV, as revealed by RT-PCR, using total RNA from the cerebellar cortex of BDV-infected, and non-infected rats, 8 weeks p.i. (Fig. 2B). As loading control, RNA-expression of the housekeeping gene GAPDH was investigated in the same samples (Fig. 2C). Statistical analysis of the optic density of Cx specific PCR bands, confirmed the BDV dependent expression changes to be significant (Figs. 2D and E). Similar experiments, with samples from 4 weeks p.i., revealed no BDV dependent changes of either Cx43, or Cx30 (data not shown).

2.3. *BDV dependent changes in expression of Cx43 and Cx30 as revealed by Western blot analysis*

As revealed on the protein level by Western blot analysis, using samples of animals 8 weeks p.i., overall Cx43 immunoreactivity was not significantly changed ($p=0.055$) by BDV infections, compared to samples of non-infected controls (Fig. 3A). Instead, an increase of those Cx43 specific bands, representing the phosphorylated active form of this molecule, could be observed. In contrast to that, immunoreactivity for Cx30 was reduced in cerebellar protein samples from BDV-infected rats, 8 weeks p.i., thereby confirming the findings on the mRNA level (Fig. 3B). In this case, the housekeeping gene β-actin, was analyzed as a loading control (Fig. 3C). Statistical analysis of the optic density of Cx specific immunoreactive bands, confirmed the BDV dependent expression changes to be significant (Fig. 3D, E, and F). Similar experiments with samples from 4 weeks p.i., revealed no BDV dependent changes of either Cx43, or Cx30 (data not shown).

2.4. *BDV dependent layer specific changes in Cx43 immunoreactivity in the rat cerebellar cortex as revealed by immunofluorescent staining*

To detect BDV dependent changes in Cx43 expression in different layers of the cerebellar cortex, patterns of Cx43 immunoreactive plaques in the cerebellar cortex of BDV-infected, and non-infected rats, was investigated by indirect immunofluorescent staining (Figs. 4A–J). In cerebellar sections of non-infected control animals, 4 weeks p.i. (Figs. 4A and C), only few, and weakly stained Cx43 immunoreactive GJ plaques were detectable in the ML, whereas in the granular layer (GL), high numbers of strongly stained Cx43 immunopositive GJ plaques, could be observed. In the brains of BDV-infected rats, 4 weeks p.i. (Figs. 4B and D), abundance of Cx43 immunoreactive GJ plaques, remained low in the ML, and was greatly diminished in the GL, as compared to non-infected controls (Figs. 4A, and C).

8 weeks p.i., in sections of non-infected animals (Fig. 4E and G), abundance of Cx43 immunoreactive GJ plaques was low in ML, and high in GL. In corresponding sections of BDV-infected rat brains (Figs. 4F and H), staining for Cx43 remained high in the GL, and revealed a massive induction in the ML. Distribution of Cx43 positive GJ plaques in the ML, suggests them to be located in radial glia cells (Fig. 4H). Changes in immunohistochemical staining intensities for Cx43 in the different layers of the cerebellar cortex were determined densitometrically, followed by statistical evaluation, confirming all described changes to be significant (Fig. 4I, and J). An overview on BDV dependent changes in immunohistochemical staining for Cx43, is also given in Table 1.

2.5. *BDV dependent layer specific changes in Cx30 immunoreactivity in the rat cerebellar cortex as revealed by immunoperoxidase staining*

Also Cx30, another astroglial Cx subtype, revealed BDV dependent spatial and temporal expression changes, as shown by immunoperoxidase staining (Figs. 5A–J). Thus, in the brain of a non-infected control animal (Figs. 5A and C), almost no Cx30 immunoreactive GJ plaques were observed in the ML, whereas in the GL, strong Cx30 specific immunoreactivity was detectable 4 weeks p.i. In BDV-infected animals (Figs. 5B and D) this pattern was not changed for the ML, however, in the GL, immunoreactivity for Cx30 was nearly entirely lost 4 weeks p.i.

In control treated animals, 8 weeks p.i., a similar pattern could be observed, with high Cx30 specific immunoreactivity in the GL, and a lack of Cx30 specific immunoreactivity in the ML (Figs. 5E and G). In BDV-infected animals at this late time point (Figs. 5F and H), Cx30 specific immunoreactivity was nearly entirely lost in the GL, and remained undetectable in the ML.

Changes in immunoperoxidase staining for Cx30 in the different layers of the cerebellar cortex, were determined densitometrically, followed by statistical evaluation, which confirmed the described changes to be significant (Figs. 5I, and J). An overview on BDV dependent changes in immunohistochemical staining for Cx30, is also given in Table 1.

2.6. *Immunofluorescent detection of BDV dependent changes in the expression of glial fibrillar acidic protein in the rat cerebellar cortex*

Since persistent BDV infection is known to result in astrogliosis, an important question was, whether changes in cerebellar astroglial GJ expression could be correlated to BDV dependent astrogliotic changes. To clarify this point, expression of the astrogliotic marker glial fibrillar acidic protein (GFAP) was analyzed in the cerebellar cortex of BDV-infected, and corresponding control animals, 4, and 8 weeks p.i. by immunofluorescent detection (Figs. 6A–E). Whereas 4 weeks p.i., staining intensity of GFAP in radial glial processes of the cerebellar cortex of BDV-infected rats was only moderately increased, as compared to non-infected animals (Figs. 6A, and B), 8 weeks p.i., this increase was much stronger (Figs. 6C, and D). A similar increase in GFAP immunoreactivity, could

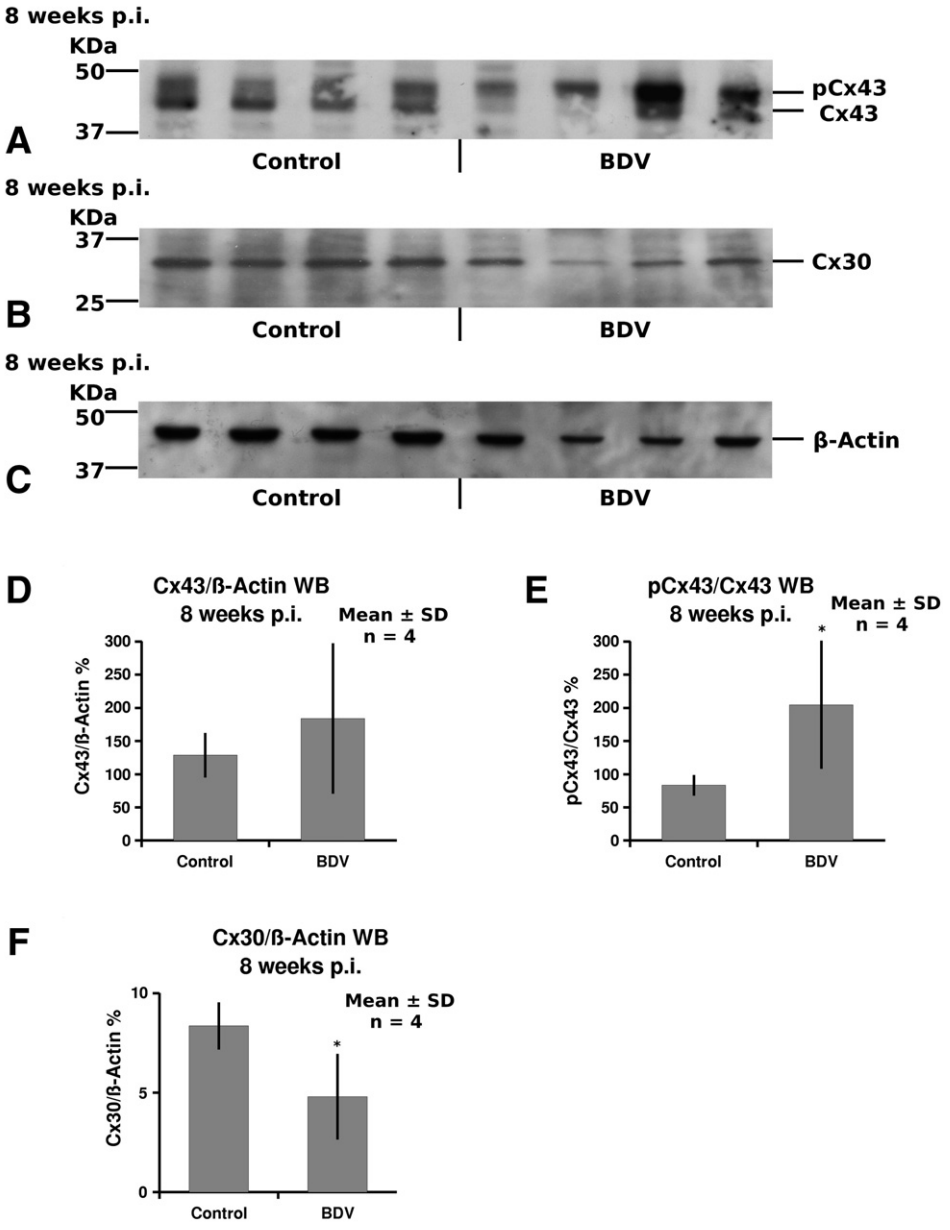

Fig. 3 – Investigation of the immunoreactivity for Cx43 and Cx30, in the cerebellar cortex of BDV-infected, and non-infected Lewis rats, 8 weeks p.i., by Western blot. (A) ECL exposure of a Western blot, for the detection of cerebellar Cx43 in whole cell extracts, from non-infected control animals, and BDV-infected rats, 8 weeks p.i. (B) ECL exposure of a Western blot, for the detection of cerebellar Cx30, in whole cell extracts from non-infected control animals, and BDV-infected rats, 8 weeks p.i. (C) ECL exposure of a Western blot, for the detection of cerebellar β-Actin, in whole cell extracts from non-infected control animals, and BDV-infected rats 8 weeks p.i. (D) Graph of a statistical evaluation, of the intensity of the Cx43 specific protein bands, shown in (A), compared to the corresponding bands of β-Actin, shown in (C). (E) Graph of the statistical evaluation, of the ratio between the intensity of the phosphorylated active form of Cx43, and the non-phosphorylated inactive form of this molecule, as shown in (A). Whereas immunoreactivity for Cx43 was not altered in the BDV-infected cerebellar cortex, a BDV dependent shift from the non-phosphorylated inactive form, to the phosphorylated active form of Cx43, could be observed. (F) Graph of the statistical evaluation of the intensity of the Cx30 specific protein bands, shown in (B), compared to the corresponding bands of β-Actin, shown in (C). Cx30 immunoreactivity is decreased in the cerebellar cortex of BDV-infected rats. Error bars = standard deviation, $^{*}p \leq 0.05$.

also be observed in astrocytes in the GL, 4, and 8 weeks p.i. (Figs. 6A–D). Thus, expression of GFAP is indeed induced in the cerebellar cortex of BDV-infected rats, suggesting a direct, or inverse correlation to the expression pattern of Cx43, or Cx30 respectively. Changes in immunofluorescent staining for GFAP in the ML of the cerebellar cortex, were also densitometrically analyzed, and statistically evaluated, confirming the described changes to be significant (Fig. 6E). An overview on BDV dependent changes in immunohistochemical staining for GFAP is given in Table 1.

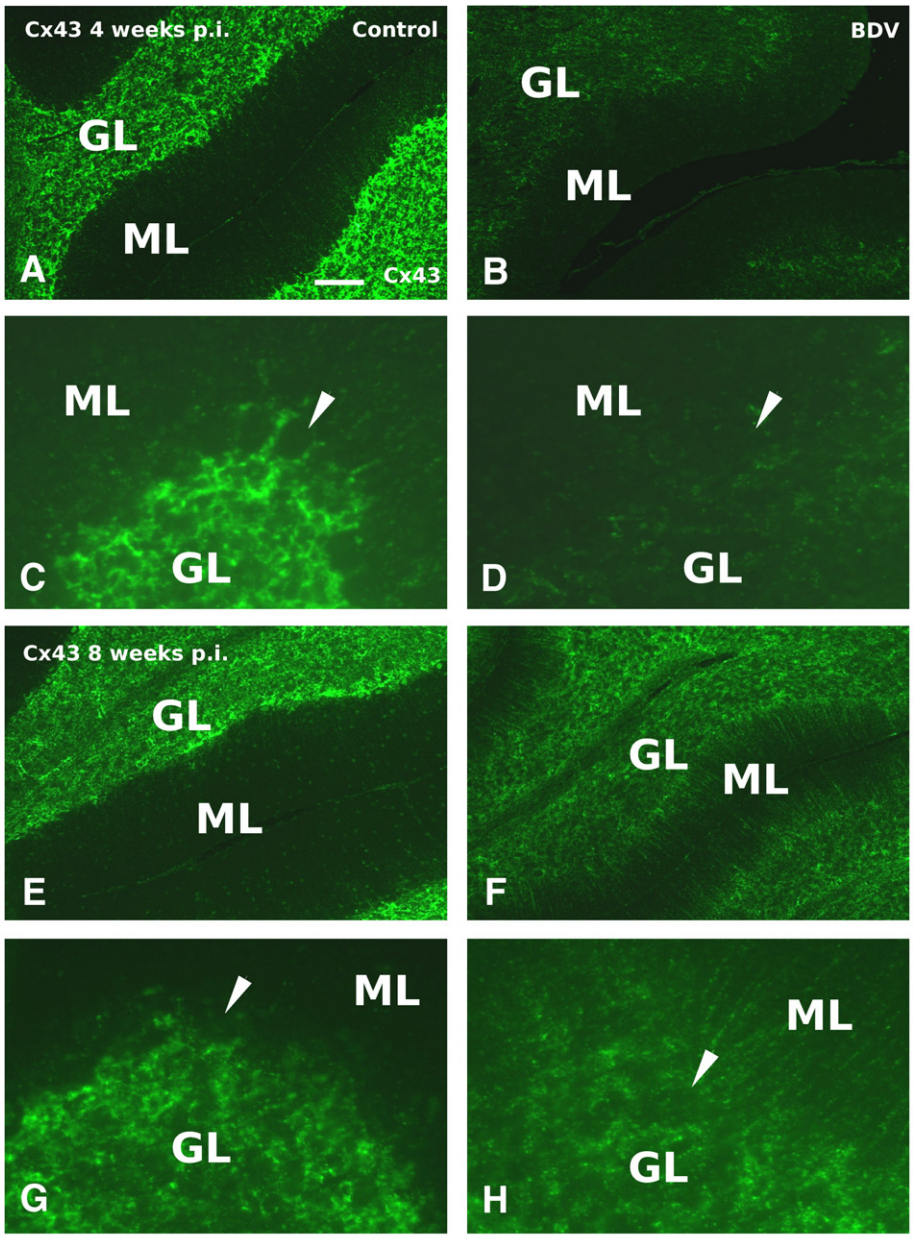
Cx43 4 weeks p.i.
Control
GL
ML
A
Cx43
BDV
GL
ML
B
ML
C
GL
ML
D
GL
Cx43 8 weeks p.i.
GL
ML
E
GL
ML
F
ML
G
GL
ML
H
GL

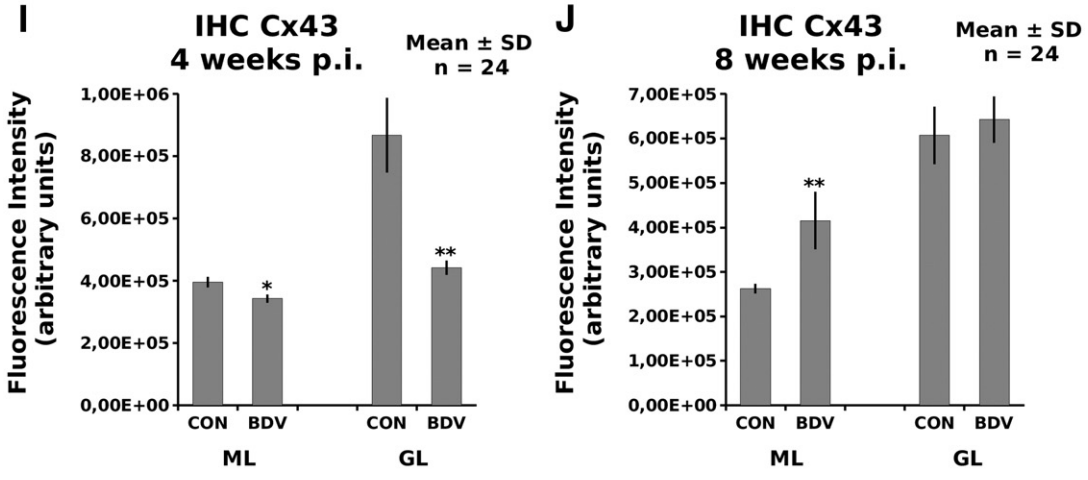
I
IHC Cx43
4 weeks p.i.
Mean ± SD
n = 24
Fluorescence Intensity
(arbitrary units)
1,00E+06
8,00E+05
6,00E+05
4,00E+05
2,00E+05
0,00E+00
*
**
CON
BDV
CON
BDV
ML
GL
J
IHC Cx43
8 weeks p.i.
Mean ± SD
n = 24
Fluorescence Intensity
(arbitrary units)
7,00E+05
6,00E+05
5,00E+05
4,00E+05
3,00E+05
2,00E+05
1,00E+05
0,00E+00
**
CON
BDV
CON
BDV
ML
GL

2.7. BDV dependent changes of functional GJ coupling in primary cerebellar astroglial cultures

To clarify, whether the BDV dependent changes in Cx expression, described above, lead also to altered functional GJ coupling, an *in vitro* system of primary cerebellar astroglial cultures was established. As shown in Figs. 7A, and B, repeated incubation of these cultures with BDV, lead to successful infection, since, compared to non-infected control cultures, BDV-infected cultures revealed increased immunoreactivity for an antibody directed to the viral BDVp40 protein. Astroglial nature of the cells used for this study, was verified by immunocytochemical staining for the astrogliotic marker protein GFAP. Both, control cultures (Fig. 7C), and BDV-infected cells (Fig. 7D) revealed strong GFAP immunoreactivity. This was accompanied by an increase in immunoreactivity for Cx43 (Figs. 7E and F), and also of Cx30 (Figs. 7G, and H). In addition, Western blot analysis revealed an increase in immunoreactivity for both, Cx43, and Cx30, as well as an increase in the phosphorylated forms of Cx43 (Inset in Figs. 7F and H). As a loading control immunoreactivity for β-actin was investigated, which was not changed at all (data not shown).

To asses BDV dependent changes in functional GJ coupling, BDV-infected primary cerebellar astroglial cultures were analyzed by the scrape loading technique, for their capability of intercellular transfer of the GJ permeant fluorescent dye Lucifer yellow (LY), to neighbouring cells. As shown in Fig. 8A, non-infected primary cerebellar astroglial cells, revealed spreading of LY to neighbouring cells. In BDV-infected cultures, intercellular spreading of LY was significantly enhanced (Figs. 8B, C).

Table 1 – Region specific changes in immunoreactivity for the astroglial gap junction proteins Cx43, and Cx30, and for the intermediate filament protein GFAP, in the BDV-infected rat cerebellar cortex

			CON	BDV
Cx43				
	4 weeks p.i.	ML	+	–
		GL	+++	+
	8 weeks p.i.	ML	+	++
		GL	+++	+++
Cx30				
	4 weeks p.i.	ML	–	–
		GL	+++	+
	8 weeks p.i.	ML	–	–
		GL	+++	+
GFAP				
	4 weeks p.i.	ML	+	++
		GL	+	++
	8 weeks p.i.	ML	+	+++
		GL	+	+++

+++ = high immunoreactivity , ++ = medium immunoreactivity, + = low immunoreactivity, – = no immunoreactivity; GL = granular layer, ML = molecular layer.

3. Discussion

The present study demonstrates BDV dependent Purkinje cell degeneration, to be associated with changes in expression, and function of astroglial GJ proteins Cx43, and Cx30, in the Lewis rat cerebellar cortex, and in primary cultures of cerebellar astroglial cells. These changes included: 1.) a global increase of Cx43 mRNA, and a decrease of the mRNA coding for Cx30, as revealed by RT-PCR. 2.) An increase in the phosphorylated active forms of Cx43 protein, and a global decrease of Cx30 protein expression, as revealed by Western blot analysis. 3.) A decrease of both Cx30, and Cx43 immunoreactivity in the GL of BDV-infected rats, 4 weeks p.i. 4.) An induction of Cx43, but not of Cx30 in the ML of BDV-infected rats, 8 weeks p.i. 5.) An induction of the astrogliotic marker protein GFAP, in ML, and GL of BDV-infected rats 4, and 8 weeks p.i. 6.) Increased functional coupling, as revealed by intercellular transfer of the GJ permeant dye LY, in BDV-infected primary cerebellar astroglial cultures.

An important point that should be discussed right at the beginning, is, that for both expression levels of Cx43, and of Cx30, depending on the particular method used, somewhat inconsistent results were obtained. Thus, although expression of Cx30 in the GL was reduced, as demonstrated by immunocytochemistry 4 weeks p.i., this was not paralleled by a decrease on either the mRNA level, or the protein level, when Western blotting and RT-PCR was applied. With regard to this point, it should be noted that the variability of the signals obtained by RT-PCR, and Western blot analysis, 4 weeks p.i., was much greater, than that observed 8 weeks p.i. A possible explanation for this finding could be that, depending on Cx turnover variable amounts of Cx protein are located in intracellular stores, such as the endoplasmic reticulum, or the Golgi apparatus. These molecules might be detected by Western blot, but not by immunocytochemistry. Also the lack of differences in Cx43 mRNA and protein detected 4 weeks p.i. by Western blot and RT-PCR, despite an

Fig. 4 – Immunofluorescent detection of Cx43, in histological sections of the cerebellar cortex, of control treated, and BDV-infected Lewis rats, 4, and 8 weeks p.i. (A, B) Overview on Cx43 immunofluorescence, in the cerebellar cortex of a control treated (A), and a BDV-infected (B) rat brain, 4 weeks p.i. (C, D) Detailed view of Cx43 immunofluorescence, in the cerebellar cortex, of a control treated (C), and a BDV-infected (D) rat brain, 4 weeks p.i. (E, F) Overview on Cx43 immunofluorescence, in the cerebellar cortex of a control treated (E), and a BDV-infected (F) rat brain, 8 weeks p.i. (G, H) Detailed view of Cx43 immunofluorescence, in the cerebellar cortex of a control treated (G), and a BDV-infected (H) rat brain, 8 weeks p.i. (I, J) Graphs of the statistical analysis, of a densitometric evaluation of the staining intensity, at 6 accidentally chosen areas, in a series of 4 immunostainings, as shown in (A–H). 4 weeks p.i., Cx43 immunoreactivity is significantly reduced in both, GL, and ML of BDV-infected animals. 8 weeks p.i., Cx43 immunoreactivity is induced, in ML, but not in GL of BDV-infected animals. Arrowhead = Purkinje neurons. GL = granular layer, ML = molecular layer, Bar represents 200 μm in A, B, E, and F, and 50 μm in C, D, G, and H. Error bars = standard deviation, $^{*}p \leq 0.05$, $^{**}p \leq 0.01$.

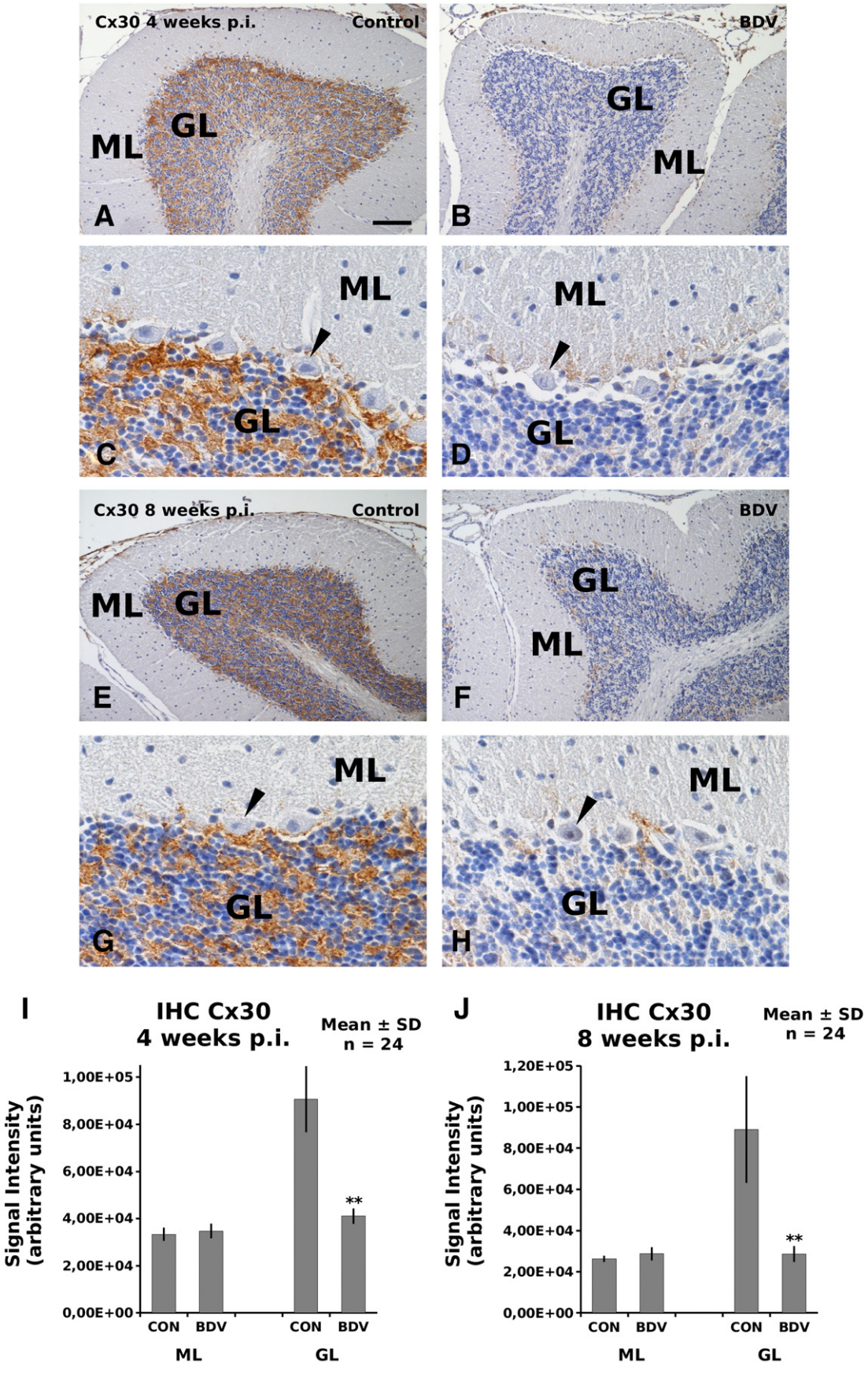
Cx30 4 weeks p.i.
Control
ML
GL
A
BDV
GL
ML
B
ML
GL
C
ML
GL
D
Cx30 8 weeks p.i.
Control
ML
GL
E
BDV
GL
ML
F
ML
GL
G
ML
GL
H
I
IHC Cx30
4 weeks p.i.
Mean ± SD
n = 24
Signal Intensity
(arbitrary units)
1,00E+05
8,00E+04
6,00E+04
4,00E+04
2,00E+04
0,00E+00
**
CON
BDV
CON
BDV
ML
GL
J
IHC Cx30
8 weeks p.i.
Mean ± SD
n = 24
Signal Intensity
(arbitrary units)
1,20E+05
1,00E+05
8,00E+04
6,00E+04
4,00E+04
2,00E+04
0,00E+00
**
CON
BDV
CON
BDV
ML
GL

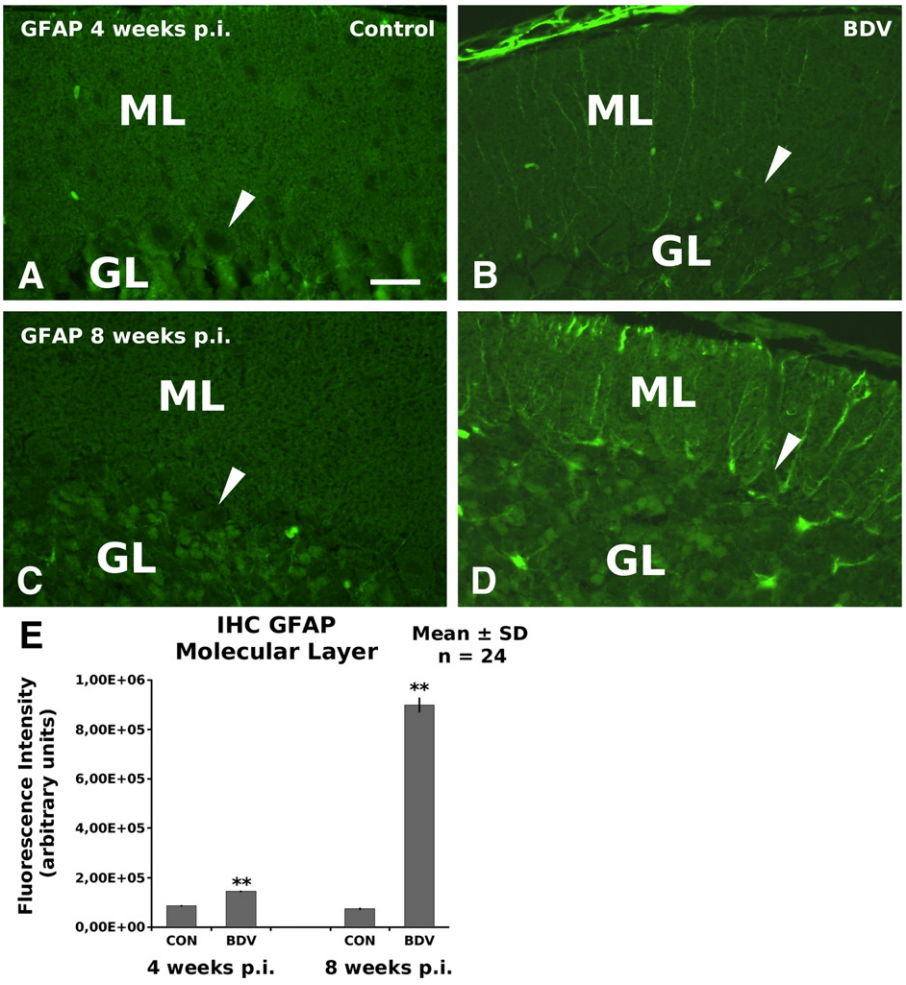

Fig. 6 – Immunofluorescent detection of the astrogliotic marker protein GFAP, in the cerebellar cortex of control treated (A, C), and BDV-infected (B, D,) Lewis rats, 4 (A, B), and 8 (C, D) weeks p.i. (E) Graph of the statistical evaluation of a densitometry, of the immunoreactivity in a series of immunostainings, as shown in (A–D). GFAP immunoreactivity is significantly induced, in the cerebellar cortex of BDV-infected rats, both, 4, and 8 weeks p.i. Arrowhead = Purkinje neurons, GL = granular layer, ML = molecular layer. Bar represents 50 μm, Error bars = standard deviation, $^{**}p \leq 0.01$.

apparent downregulation of this Cx in the GL as revealed by immunocytochemistry, could be explained by a similar way.

Another discrepant finding with regard to different methods applied was also, that, although overall Cx43 protein expression, as detected by Western blot analysis, was not increased 8 weeks p.i., Cx43 immunoreactivity, as shown by immunohistochemistry, was induced in the ML at this time point. This could be explained by the fact, that the regionally restricted changes observed in ML by immunohistochemical staining, is probably too week to result in a significant change in total Cx43 expression, as detected in the protein samples from the whole cerebellar cortex, as used for Western blot analysis.

A special finding of the present study was, that the global increase in Cx43 mRNA, detected by RT-PCR, at least with the

Fig. 5 – Immunoperoxidase detection of Cx30 specific immunoreactivity, in the cerebellar cortex of control treated, and BDV-infected Lewis rats, 4, and 8 weeks p.i. (A, B) Overview on Cx30 immunoreactivity in the cerebellar cortex, of a control treated (A), and a BDV-infected (B) rat brain, 4 weeks p.i. (C, D) Detailed view of Cx30 immunofluorescence, in the cerebellar cortex of a control treated (C), and a BDV-infected (D) rat brain, 4 weeks p.i. (E, F) Overview on Cx30 immunofluorescence, in the cerebellar cortex of a control treated (E), and a BDV-infected (F) rat brain, 8 weeks p.i. (G, H) Detailed view of Cx30 immunoreactivity, in the cerebellar cortex of a control treated (G), and a BDV-infected (H) rat brain, 8 weeks p.i. (I, J) Graphs of the statistical analysis of a densitometric evaluation, of the staining intensity at 6 accidentally chosen areas, in a series of 4 immunostainings, as shown in (A–H). Cx30 immunoreactivity is significantly reduced in GL of BDV-infected rats, 4, and 8 weeks p.i. Arrowhead = Purkinje neurons. GL = granular layer, ML = molecular layer, Bar represents 200 μm in A, B, E, and F, and 50 μm in C, D, G, and H. Error bars = standard deviation, $^{**}p \leq 0.01$.

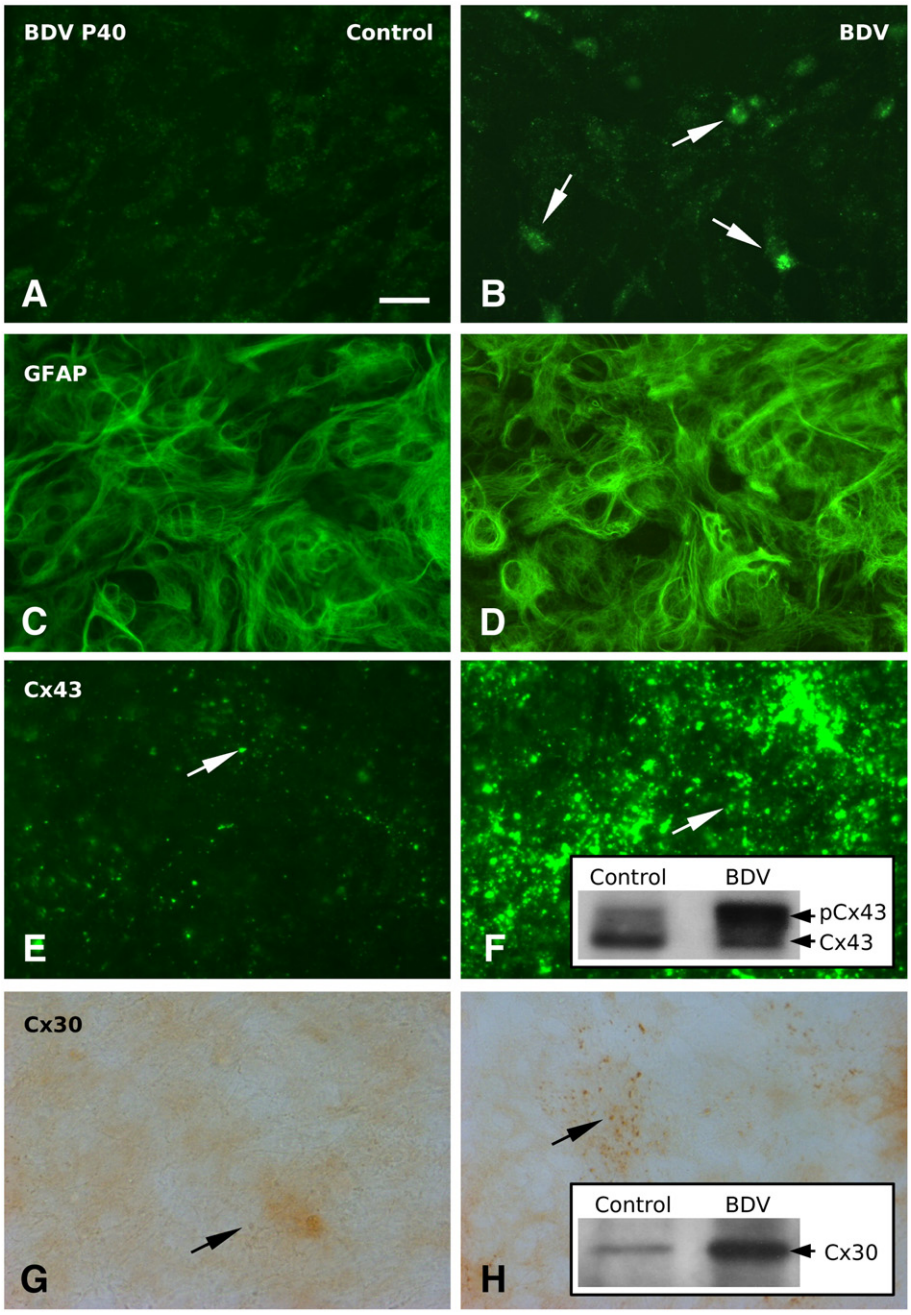

Fig. 7 – Immunohistochemical characterization of non-infected, and BDV-infected primary cerebellar astroglial cultures *in vitro*. (A, B) Immunofluorescent detection of BDV-p40 in non-infected control cultures (A), and in BDV-infected (B) primary cerebellar astroglial cells. (C, D) Immunofluorescent detection of GFAP, in non-infected controls (C), and in BDV-infected (D) cultures of primary cerebellar astroglial cells. (E, F) Immunofluorescent detection of Cx43, in non-infected controls (E), and in BDV-infected cultures (F) of primary cerebellar astrocytes (Inset: Western blot analysis for the detection of Cx43, in similar cultures as shown in E, and F). (G, H) Immunoperoxidase detection of Cx30 in non-infected controls (G), and in BDV-infected (H) cultures of primary cerebellar astrocytes (Inset: Western blot analysis for the detection of Cx30 in similar cultures as shown in G, and H). Both, total immunoreactivity for Cx43, and Cx30, as well as for the phosphorylated active forms of Cx43, were distinctly increased in BDV-infected primary cerebellar astroglial cultures, as compared to non-infected controls. Bar represents 20 μm.

comparable small sample numbers used, did not translate into a statistically significant increase in overall cerebellar Cx43 protein, as revealed by Western blotting. In contrast, a relative increase of the phosphorylated active forms of Cx43, could be observed. Increased Cx43 phosphorylation could also be observed in primary cerebellar astroglial cultures, suggesting this mechanism to be a key factor for BDV dependent changes in functional coupling. From the literature it is known, that serin phosphorylation activates GJ channels formed by Cx43, due to a higher open probability (for a review

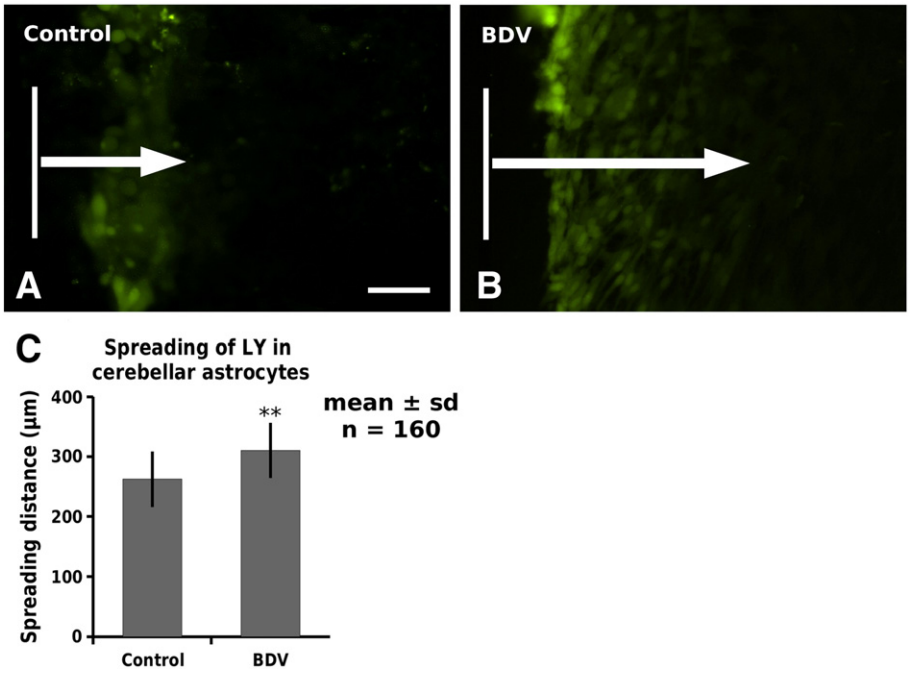

Fig. 8 – Functional coupling, in BDV-infected, and control treated primary cerebellar astroglial cells, as revealed by intercellular spreading of the GJ permeant fluorescent dye LY, after scrape loading. (A) Scrape loading experiment, for the detection of LY dye transfer in non-infected controls. (B) Similar experiment with BDV-infected primary cerebellar astroglial cells. (C) Graph of the statistical evaluation, of a series of scrape loading experiments, as depicted above. Dye spreading is significantly increased in BDV-infected primary cerebellar astrocytes. Bar represents 100 μm in A, and B. LY = Lucifer Yellow, Error bars = standard deviation. $^{**}p \leq 0.01$.

see Moreno and Lau (1996)). Therefore, the BDV dependent increase in Cx43 phosphorylation observed here *in vivo*, was in accordance to the *in vitro* finding of an increased dye transfer rate in BDV-infected primary astroglial cultures. The fact that persistent BDV infections lead to changes in Cx43 phosphorylation, clearly distinguishes this condition from other disease related changes in GJ coupling, such as protozoan or bacterial infections, which are not accompanied by changes in Cx43 phosphorylation (Campos de Carvalho et al., 1998; Esen et al., 2007).

Expression of Cx43 mRNA, and protein in the postnatal cerebellar cortex, is well established (Micevych and Abelson, 1991; Åberg et al., 1999), and also the expression of Cx30 in the GL of the cerebellar cortex, has already been reported (Condorelli et al., 2002). In addition, changes in astroglial Cx expression have been already demonstrated during bacterial, and protozoan infections (Campos de Carvalho et al., 1998; Esen et al., 2007), whereas information on the effects of persistent viral infections, have been reported only very recently (Fatemi et al., 2008; Eugenin and Berman, 2007). Thus, intrauterine infections with the Influenza virus, during the second trimester of pregnancy, lead to long lasting changes in astroglial GJs in the offsprings' brains (Fatemi et al., 2008). Also during brain infections with the human immunodeficiency virus, astroglial GJs seem to be able to transmit proapoptotic signals from infected to non-infected astrocytes, probably amplifying the negative consequences of the infection (Eugenin and Berman, 2007). This suggests, that also the changes in astroglial Cx expression reported here, could contribute to BDV dependent Purkinje cell degeneration by similar mechanisms. On the other hand, it has been reported by previous studies, that in mice with a heterozygous defect for Cx43, ischemia dependent neuronal apoptosis is increased, arguing for a protective role of BDV dependent changes in cerebellar astroglial GJs. Even more, since in the same mice, Cx30 is upregulated in the areas of neuronal damage, probably compensating the reduction in Cx43 (Nakase et al., 2003).

Changes in astroglial Cx expression are often associated with reactive astrogliosis, as it has been described for BDV dependent neuron degeneration (Carbone et al., 1989, 1991). We have investigated this for the cerebellar cortex. However, the BDV dependent induction of the astrogliotic marker GFAP, in both GL, and ML, did not correlate with the BDV dependent changes in the expression of Cx43, and Cx30. This has also been described for kainate-induced neurodegeneration in the rat brain, where the expression of astroglial Cxs was unaffected, despite a massive induction of GFAP (Söhl et al., 2000). In the present study, only the induction of GFAP in radial glia, supported a direct relationship between astrogliosis, and an upregulation of Cx43. Nevertheless, the dramatic loss of Cx30 in the GL of BDV-infected rats, 4, and 8 weeks p.i., argues for an important role of astroglial GJs during BDV dependent neurodegeneration. Mechanistic support for this comes from studies with knockout mice, with an astrocyte-specific deletion of Cx43, where the lack of Cx43 in astrocytes, did not lead to a gross neurodegeneration *per se* (Theis et al., 2003). However, these animals demonstrated increased neuronal vulnerability to global brain ischemia (Nakase et al., 2004).

Since both dentate gyrus granule cells and Purkinje neurons are amongst the neurons with increased stress vulnerability (Yamaoka et al., 1993; Welsh et al., 2002), virus dependent changes in astroglial gap junction coupling could play a role for the slowly progredient neurodegeneration during persistent BDV infection.

Despite the subacute course of the disease after neonatal BDV infection, an inflammatory response has nevertheless been reported (Sauder et al., 2000; Stitz et al., 2002), leading to an activation of microglial cells (Weissenböck et al., 2000; Ovanesov et al., 2006), and the release of proinflammatory cytokines, like interleukin-6, tumor necrosis factor α, as well as interleukin-1α, and -1β (Sauder and de La Torre, 1999). However, microglial activation, and the resulting release of tumor necrosis factor α, interleukin-1β, interleukin-6, and interferon-γ, have been shown to reduce astroglial Cx43 expression, and functional coupling (Faustmann et al., 2003; Hinkerohe et al., 2005; Même et al., 2006). Together, these findings suggest, that the release of these factors might also be involved in BDV dependent changes of astroglial Cx expression, reported in the present study.

An important question with regard to BDV dependent changes in cerebellar Cx expression is, whether these changes lead to altered functional coupling. Due to biological safety reasons, we have addressed this question in an *in vitro* system of primary cerebellar astroglial cultures, that have been repeatedly infected with the BDV. By this, an induction of Cx43, and of Cx30 expression, as well as of Cx43 phosphorylation occurs in conjunction with increased spreading of the GJ permeant dye LY. Thus, in contrast to the *in vivo* situation, an upregulation of Cx30 was observed in cultured primary cerebellar astrocytes. This clearly demonstrates, that BDV does not only affect Cx expression, but changes also functional GJ coupling in astroglial cells. However, since the observed *in vitro* effects do not match the changes in Cx expression observed *in vivo*, the relevance of these findings with regard to the *in vivo* situation remains still questionable.

In a previous study, we could demonstrate, that expression and function of astroglial Cxs are also affected by BDV in the hippocampal formation (Köster-Patzlaff et al., 2007). Comparing these results to the findings of the present study, some important similarities and differences can be observed, suggesting BDV dependent changes in astroglial GJ coupling, to be highly brain region specific. Thus, an induction of Cx43, as well as of Cx30 could be seen in the dentate gyrus of the hippocampal formation, whereas in the CA3 region, Cx43 was reduced, and Cx30 is increased (Köster-Patzlaff et al., 2007). Therefore BDV leads to an upregulation of Cx43 in both, the cerebellar cortex, and the hippocampal formation, whereas Cx30 is induced in the hippocampal formation, but repressed in the cerebellar cortex, obviously reacting in an opposite manner in both brain regions.

In conclusion, the present study is the first one, to demonstrate BDV dependent changes in cerebellar astroglial GJ expression in the Lewis rat brain *in vivo*, and of functional astroglial GJ coupling *in vitro*. Together with the previously reported changes in the hippocampal formation, it completes the view on the role of this important regulatory network during BDV dependent neurodegeneration.

4. Experimental procedures

4.1. *Animal care and viral infections*

Animal experiments were done with permission of the government of Lower Saxony (Reference nr.: 509.42502/01-40.03). Pregnant Lewis rats, purchased by Charles River (Sulzfeld, Germany), were kept in standard cages with free access to food, and water at a 12 h/12 h dark/light cycle, at 20 °C. For viral infections, 30 μl of a brain homogenate, representing a total of 1×10^4 focus forming units of the 5th brain passage of BDV He/80 strain RW98ub rat adapted (kindly provided by Dr. Peter Staeheli, Freiburg), was injected intracranially into the right hemisphere of newborn Lewis rat pups, within 12 h following birth. Corresponding control animals, were injected with similar amounts of a brain homogenate, from non-infected animals. Either 4 or 8 weeks p.i., animals were killed by nitrogen intoxication, with the brains being removed, and shock frozen on dry ice immediately. Brains were dissected midsagitally, and stored at −80 °C. In order to allow statistical evaluation, for every experimental value, at least four independent samples were analyzed.

4.2. RT-PCR

Left cerebellar hemispheres of four animals, were cut into 500 μm transverse brain slices on a Frigomobil (Reichert & Jung, Nußloch, Germany), total RNA of which, was isolated by Trifast (Peqlab, Erlangen, Germany), and purified with DNase I (Invitrogen, Karlsruhe, Germany). First strand cDNA synthesis was carried out with random hexamer primers (Fermentas, St. Leon-Rot, Germany), and RevertAid M-MuLV reverse transcriptase (Fermentas, St. Leon-Rot, Germany), using 1 μg of total RNA. PCR amplification was performed in a Mastercycler gradient (Eppendorf, Hamburg, Germany), using a commercial PCR Master Mix (Fermentas, St. Leon-Rot, Germany), with the primary reaction containing 1 μl of cDNA, 12.5 μl PCR Master Mix, 0.2 μmol/l of each primer in a total volume of 25 μl. For detection of BDV, the following primers were used: BDV-p40: (forward 5′-ACG CCC AGC CTT GTG TTT CT-3′, reverse 5′-AAT TCT TTA CCT GGG GAC TCA A-3′; fragment length 449 bp). Cycling conditions involved an initial 2′ denaturation step at 95 °C, followed by 40 cycles, each consisting of a 30″ denaturation step at 94 °C, a 45″ annealing step at 58 °C, and a 1′ extension step at 72 °C. Reactions were terminated by a final elongation step of 10′ at 72 °C. Reaction products obtained were analyzed by agarose gel electrophoresis, followed by ethidium bromide staining, and subsequent fluorescent detection. In order to enhance detection specificity, an additional round of nested PCR reactions was performed, for which each sample contained 1 μl of the primary PCR template, 11 μl PCR Master Mix, 0.2 μmol/l of each primer, at a total volume of 25 μl. Primer pairs were as follows: BDV-p40 nested: (forward 5′-CTC GTG AAT CTT ACC TGT CGA CG-3′; reverse: 5′-TCC TGC TTT AAT CTT AGA TGA CG-3′; fragment length 188 bp). Nested cycling conditions, were as described for the primary amplification, with the exception that only 30 cycles were used for amplification. Again, reaction products were analyzed by agarose gel electrophoresis. Cx43 and Cx30 mRNAs were

detected using the following primer pairs: Cx43 (forward: 5′-TCC TTG GTG TCT CTC GCT TTG A-3′; reverse: 5′-CTG GCT CTG CTG GAA GGT CGT T-3′; fragment length 456 bp) and Cx30 (forward: 5′-TTC CAG TTC ACC TCA CAC GG-3′; reverse: 5′-ACC ACG AGG ATC ATG ACT CG-3′; fragment length 373 bp). Cycle conditions included an initial step of 94 °C for 3′, 35 amplification cycles (94 °C 1′, 60 °C 1.5′, 72 °C 1.5′), and a final elongation step at 72 °C, for 10′. As a loading control, the housekeeping gene glyceraldehyde-3-phosphate dehydrogenase (GAPDH) was detected, using the following primer pairs: GAPDH: (forward 5′-CCT TCA TTG ACC TCA ACT ACA T-3′; reverse 5′-CCA AAG TTG TCA TGG ATG ACC-3′; fragment length 398 bp). Cycling conditions for amplification of Cx43, Cx30, and GAPDH, were all chosen in order to cover the exponential phase of amplification, to allow semiquantitative comparison of intensities of the obtained PCR bands. Intensity of PCR bands of 4 independent experiments, was measured densitometrically, and mean values and standard deviations were calculated. Significance was analyzed with Student's two-tailed *t*-test, and alternatively by the Wilcoxon rank-sum test.

4.3. *Western blot analysis*

Left cerebellar hemispheres of four animals, as specified above, were cut into 500 μm transverse brain slices, on a Frigomobil (Reichert & Jung, Nußloch, Germany). Each slice was thawed in 500 μl of ice chilled homogenation buffer, containing 25 mmol/l Tris pH 7.5, 1 mmol/l EDTA, 1 % SDS (w/v), 0.5 mmol/l DTT and 40 μl/ml Protease Inhibitor Cocktail (Roche, Basel, Switzerland). After mechanical homogenation, and sonication at 4 °C, protein concentrations were determined according to Bradford (1976). Protein samples of 10 μg were size fractionated in electrophoresis sample buffer (0.5 mmol/l TRIS/HCl pH 6.8, 2% SDS (w/v), 10% glycerol (v/v), 5% β-mercaptoethanol (v/v) and 0.001% bromophenol blue (w/v)), by SDS-PAGE (Laemmli, 1970). Proteins were blotted onto polyvinylidene difluoride membranes (PVDF; Roth, Karlsruhe, Germany), which were then blocked for 8 h at 4 °C in 3 % (w/v) nonfat dry milk in TRIS-buffered saline, with 0.01 % Tween 20 (TBST). Blots were probed with antibodies against Cx30 (rabbit polyclonal; dilution 1:80, Invitrogen, Carlsbad, California, USA), or Cx43 (mouse monoclonal, dilution 1:300; Invitrogen, Carlsbad, California, USA), diluted in TBST with 0.1% nonfat dry milk. Primary antibodies were detected by incubation with appropriate peroxidase conjugated secondary antibodies (goat anti-rabbit, dilution 1:20.000; goat anti-mouse, dilution 1:10.000; both from Pierce, Rockford, Illinois, USA), which were visualized by exposing CLXposure X-ray films (Pierce, Rockford, Illinois, USA), during the application of an enhanced chemiluminescence detection solution (Pierce ECL Western Blotting Substrate, Pierce, Rockford, Illinois, USA). After development, and fixation of the films, ECL-signals were scanned, and were evaluated densitometrically for quantification, using the Metamorph image analysis software (Molecular Devices, Sunnyvale, California, USA). For a loading control, blots were stripped, and reprobed with an antibody directed to β-actin (mouse monoclonal, dilution 1:5000; Sigma-Aldrich, Steinheim, Germany) being detected as described above. Intensity of Western blot signals of 4 independent experiments was measured densitometrically, and mean values, and standard deviations were calculated. Significance was analyzed with Student's two-tailed *t*-test, and alternatively by the Wilcoxon rank-sum test. As one would expect, *p*-values obtained by both tests were basically the same.

4.4. *Immunocytochemistry*

Frozen samples of the right cerebellar hemispheres of 4 control treated, and 4 BDV-infected animals, were fixed for 10′ by 4% paraformaldehyde (PFA) in phosphate-buffered saline (PBS), at room temperature, and were subsequently embedded into paraffin. Samples were then cut into 5 μm thick sagittal sections on a rotation microtome, and classified according to Paxinos and Watson (1998). Sections used in this study were all taken from a region 3 to 6 mm lateral to the midline, with only the rostral foliae being photographically evaluated. After deparaffination, and rehydration by a sequence of xylol and solutions with decreasing ethanol content, sections were pretreated for 30′ with a target retrieval buffer (pH 6.2, Dako, Glostrup, Denmark) at 95 °C. The primary antibody directed to Cx30 (rabbit polyclonal, dilution 1:50; Invitrogen, Carlsbad, CA, USA), was applied overnight at 4 °C. For visualization of Cx30 immunoreactivity, sections were incubated with a goat anti-rabbit/HRP secondary antibody (dilution 1:500, Pierce, Rockford, IL, USA), and detected by staining with di-amino benzidine (DAB+; Dako, Glostrup, Denmark). Counterstain was performed with hematoxylin. After dehydration, sections were covered with Entellan (Merck, Darmstadt, Germany). Alternatively Cx43 immunoreactivity (mouse monoclonal, Invitrogen, Carlsbad, California, USA, dilution 1:100) was detected fluorescently by the ARK-CSAII-kits (Dako, Glostrup, Denmark), according to the manufacturers' instructions, with the slides being covered by a fluorescence mounting medium (DAKO, Glostrup, Denmark), under glass cover slips. Virus dependent astrogliosis was detected by a primary antibody, directed to GFAP (rabbit polyclonal, ready-to-use, Dako, Glostrup, Denmark), and a fluorescence coupled secondary antibody (goat anti-rabbit, dilution 1:500, Invitrogen, Carlsbad, California, USA). For all immunocytochemical stainings, control reactions in the absence of primary antibodies were found to be negative. Microscopic evaluation was performed with an Axiophot microscope, equipped with epifluorescence, and an Axiocam System for image acquisition (Carl Zeiss, Jena, Germany). Images for every experimental series were obtained under standardized illumination conditions, with fixed camera settings, in order to allow direct quantification. The observed changes in Cx expression were quantified by densitometric evaluation of the Cx specific staining in 6 randomly chosen fields of standardized size, for each of the investigated layers, on 4 sections, of 4 animals analyzed, using the Metamorph image analysis software (Molecular Devices, Sunnyvale, CA, USA). The obtained values were statistically analyzed by Student's two-tailed *t*-test ($p<0.05$).

4.5. *Cell culture*

Primary cerebellar astroglial cultures, were obtained as described earlier (McCarthy and de Vellis, 1980; Reuss et al., 1998). Cerebellar tissue samples from newborn Lewis rat pups, were dissected and collected in ice-cold Hanks' balanced salt solution (HBSS). Tissue pieces were dissociated by trituration with a fire-polished Pasteur pipette. Following centrifugation, the pellet was resuspended in Dulbecco's Modified Eagle's Medium (DMEM),

supplemented with 10% fetal calf serum, penicillin (50 IU/ml), and streptomycin (50 μg/ml), (all from Gibco-BRL, Berlin, Germany). The cell suspension out of 6 cerebellae, was seeded on a 75 cm^2 tissue culture flask (Costar, Cambridge, MA, USA), coated with poly-L-lysine (Sigma-Aldrich, Steinheim, Germany). Cells were immediately infected with BDV, by adding 10 μl of a brain homogenate, containing ca. 0.33×10^4 focus forming units of the 5th brain passage of BDV strain He/80 RW98ub, rat adapted (kindly provided by Dr. Peter Staeheli, Freiburg) to the cell culture flask. Control cultures were treated with a similar brain homogenate from non-infected animals. After 3 days, cells were washed 3 times with ice-cold HBSS, to reduce oligodendrocyte numbers, and were subsequently grown to confluency in DMEM as stated above. The culture medium was changed every other day, with the cultures being reinfected as stated above. After 2 weeks, cells were dissociated by trypsinization, with the resulting cell suspension being seeded either on 10 cm cell culture grade petri dishes (Beckton-Dickinson, Heidelberg, Germany) for scrape loading (see below), or on 12 mm glass cover slips in multiwell plates for immunocytochemical analysis of BDV p40, the astrocyte-specific marker GFAP, and Cx43 and Cx30 as described above. For Western blot analysis astrocytes were cultured on 10 cm cell culture grade plastic petri dishes (Becton, Dickinson, Heidelberg, Germany), and were harvested and analyzed as described above.

4.6. *Scrape loading*

For scrape loading (Doble et al., 1996), confluent monolayers of primary cerebellar astroglial cells were washed three times with sterile saline (0,9% NaCl), and were covered with 1 mg/ml LY-CH (Sigma-Aldrich, Steinheim, Germany) in sterile saline at 37 °C. For each petri dish, four parallel scrapes were set in the monolayer with a scalpel blade, with the dye solution being removed after 2′, and the cells being washed three times with sterile saline. 4′ after setting the scrapes, cells were fixed for 10′ with an ice-cold solution of 1% PFA in sterile saline to stop further spreading of the dye. After three washes with sterile saline, dye spreading was documented photographically, using an inverse microscope equipped with epifluorescence (Zeiss, Jena, Germany), with standardized illumination conditions, and camera settings. For statistical evaluation, distances of dye spreading were measured at 10 locations at each of four scrapes in 4 independent experiments. Significance was analyzed by Student's two-tailed *t*-test ($p < 0.05$).

Acknowledgments

This work has been supported by the Deutsche Forschungsgemeinschaft (DFG — Center for the Molecular Physiology of the Brain). We thank Maren Sender, and Birgit Smith for their excellent technical assistance, and Cyrilla Maelicke for proofreading of this manuscript.

REFERENCES

Åberg, N.D., Rönnbäck, L., Eriksson, P.S., 1999. Connexin43 mRNA and protein expression during postnatal development of defined brain regions. Brain Res. Dev. Brain Res. 115, 97–101.

Altevogt, B.M., Paul, D.L., 2004. Four classes of intercellular channels between glial cells in the CNS. J. Neurosci. 24, 4313–4323.

Bautista, J.R., Schwartz, G.J., de la Torre, J.C., Moran, T.H., Carbone, K.M., 1994. Early and persistent abnormalities in rats with neonatally acquired Borna disease virus infection. Brain Res. Bull. 34, 31–40.

Belliveau, D.J., Naus, C.C., 1995. Cellular localization of gap junction mRNAs in developing rat brain. Dev. Neurosci. 17, 81–96.

Billaud, J.N., Ly, C., Phillips, T.R., de la Torre, J.C., 2000. Borna disease virus persistence causes inhibition of glutamate uptake by feline primary cortical astrocytes. J. Virol. 74, 10438–10446.

Bradford, M.M., 1976. A rapid and sensitive method for the quantitation of microgram quantities of protein utilizing the principle of protein-dye binding. Anal. Biochem. 72, 248–254.

Campos de Carvalho, A.C., Roy, C., Hertzberg, E.L., Tanowitz, H.B., Kessler, J.A., Weiss, L.M., Wittner, M., Dermietzel, R., Gao, Y., Spray, D.C., 1998. Gap junction disappearance in astrocytes and leptomeningeal cells as a consequence of protozoan infection. Brain Res. 790, 304–314.

Carbone, K.M., Trapp, B.D., Griffin, J.W., Duchala, C.S., Narayan, O., 1989. Astrocytes and Schwann cells are virus-host cells in the nervous system of rats with Borna disease. J. Neuropathol. Exp. Neurol. 48, 631–644.

Carbone, K.M., Moench, T.R., Lipkin, W.I., 1991. Borna disease virus replicates in astrocytes, Schwann cells and ependymal cells in persistently infected rats: location of viral genomic and messenger RNAs by in situ hybridization. J. Neuropathol. Exp. Neurol. 50, 205–214.

Charles, A.C., Naus, C.C., Zhu, D., Kidder, G.M., Dirksen, E.R., Sanderson, M.J., 1992. Intercellular calcium signaling via gap junctions in glioma cells. J. Cell Biol. 118, 195–201.

Condorelli, D.F., Mudò, G., Trovato-Salinaro, A., Mirone, M.B., Amato, G., Belluardo, N., 2002. Connexin-30 mRNA is up-regulated in astrocytes and expressed in apoptotic neuronal cells of rat brain following kainate-induced seizures. Mol. Cell. Neurosci. 21, 94–113.

Dermietzel, R., Gao, Y., Scemes, E., Vieira, D., Urban, M., Kremer, M., Bennett, M.V., Spray, D.C., 2000. Connexin43 null mice reveal that astrocytes express multiple connexins. Brain Res. Brain Res. Rev. 32, 45–56.

Doble, B.W., Chen, Y., Bosc, D.G., Litchfield, D.W., Kardami, E., 1996. Fibroblast growth factor-2 decreases metabolic coupling and stimulates phosphorylation as well as masking of connexin43 epitopes in cardiac myocytes. Circ. Res. 79, 647–658.

Drake-Baumann, R., Seil, F.J., 1999. Influence of functional glia on the electrophysiology of Purkinje cells in organotypic cerebellar cultures. Neuroscience 88, 507–519.

Eiberger, J., Kibschull, M., Strenzke, N., Schober, A., Büssow, H., Wessig, C., Djahed, S., Reucher, H., Koch, D.A., Lautermann, J., Moser, T., Winterhager, E., Willecke, K., 2006. Expression pattern and functional characterization of connexin29 in transgenic mice. Glia 53, 601–611.

Eisenman, L.M., Brothers, R., Tran, M.H., Kean, R.B., Dickson, G.M., Dietzschold, B., Hooper, D.C., 1999. Neonatal Borna disease virus infection in the rat causes a loss of Purkinje cells in the cerebellum. J. Neurovirol. 5, 181–189.

Esen, N., Shuffield, D., Syed, M.M., Kielian, T., 2007. Modulation of connexin expression and gap junction communication in astrocytes by the gram-positive bacterium *S. aureus*. Glia 55, 104–117.

Eugenin, E.A., Berman, J.W., 2007. Gap junctions mediate human immunodeficiency virus-bystander killing in astrocytes. J. Neurosci. 27, 12844–12850.

Farahani, R., Pina-Benabou, M.H., Kyrozis, A., Siddiq, A., Barradas, P.C., Chiu, F.C., Cavalcante, L.A., Lai, J.C., Stanton, P.K.,

Rozental, R., 2005. Alterations in metabolism and gap junction expression may determine the role of astrocytes as "good samaritans" or executioners. Glia 50, 351–361.
Fatemi, S.H., Folsom, T.D., Reutiman, T.J., Sidwell, R.W., 2008. Viral regulation of aquaporin 4, connexin 43, microcephalin and nucleolin. Schizophr. Res 98, 163–177.
Faustmann, P.M., Haase, C.G., Romberg, S., Hinkerohe, D., Szlachta, D., Smikalla, D., Krause, D., Dermietzel, R., 2003. Microglia activation influences dye coupling and Cx43 expression of the astrocytic network. Glia 42, 101–108.
Froes, M.M., de Carvalho, A.C., 1998. Gap junction-mediated loops of neuronal-glial interactions. Glia 24, 97–107.
Hinkerohe, D., Smikalla, D., Haghikia, A., Heupel, K., Haase, C.G., Dermietzel, R., Faustmann, P.M., 2005. Effects of cytokines on microglial phenotypes and astroglial coupling in an inflammatory coculture model. Glia 52, 85–97.
Hornig, M., Briese, T., Lipkin, W.I., 2003. Borna disease virus. J. Neurovirol. 9, 259–273.
Köster-Patzlaff, C., Hosseini, S.M., Reuss, B., 2007. Persistent Borna Disease Virus infection changes expression and function of astroglial gap junctions *in vivo* and *in vitro*. Brain Res. 1184, 316–332.
Laemmli, U.K., 1970. Cleavage of structural proteins during the assembly of the head of bacteriophage T4. Nature 227, 680–685.
Lancaster, K., Dietz, D.M., Moran, T.H., Pletnikov, M.V., 2006. Abnormal social behaviors in young and adult rats neonatally infected with Borna disease virus. Behav. Brain Res. 176, 141–148.
McCarthy, K.D., de Vellis, J., 1980. Preparation of separate astroglial and oligodendroglial cell cultures from rat cerebral tissue. J. Cell Biol. 85, 890–902.
Même, W., Calvo, C.F., Froger, N., Ezan, P., Amigou, E., Koulakoff, A., Giaume, C., 2006. Proinflammatory cytokines released from microglia inhibit gap junctions in astrocytes: potentiation by beta-amyloid. FASEB J. 20, 494–496.
Meshul, C.K., Seil, F.J., Herndon, R.M., 1987. Astrocytes play a role in regulation of synaptic density. Brain Res. 402, 139–145.
Micevych, P.E., Abelson, L., 1991. Distribution of mRNAs coding for liver and heart gap junction proteins in the rat central nervous system. J. Comp. Neurol. 305, 96–118.
Moreno, A.P., Lau, A.F., 1996. Gap junction channel gating modulated through protein phosphorylation. Prog. Biophys. Mol. Biol. 94, 107–119.
Müller, T., Möller, T., Neuhaus, J., Kettenmann, H., 1996. Electrical coupling among Bergmann glial cells and its modulation by glutamate receptor activation. Glia 17, 274–284.
Nagy, J.I., Patel, D., Ochalski, P.A., Stelmack, G.L., 1999. Connexin30 in rodent, cat and human brain: selective expression in gray matter astrocytes, co-localization with connexin43 at gap junctions and late developmental appearance. Neuroscience 88, 447–468.
Nagy, J.I., Li, X., Rempel, J., Stelmack, G., Patel, D., Staines, W.A., Yasumura, T., Rash, J.E., 2001. Connexin26 in adult rodent central nervous system: demonstration at astrocytic gap junctions and colocalization with connexin30 and connexin43. J. Comp. Neurol. 441, 302–323.
Nagy, J.I., Ionescu, A.V., Lynn, B.D., Rash, J.E., 2003. Coupling of astrocyte connexins Cx26, Cx30, Cx43 to oligodendrocyte Cx29, Cx32, Cx47: implications from normal and connexin32 knockout mice. Glia 44, 205–218.
Nakase, T., Fushiki, S., Naus, C.C., 2003. Astrocytic gap junctions composed of connexin 43 reduce apoptotic neuronal damage in cerebral ischemia. Stroke 34, 1987–1993.
Nakase, T., Söhl, G., Theis, M., Willecke, K., Naus, C.C., 2004. Increased apoptosis and inflammation after focal brain ischemia in mice lacking connexin43 in astrocytes. Am. J. Pathol. 164, 2067–2075.
Naus, C.C., Bani-Yaghoub, M., 1998. Gap junctional communication in the developing central nervous system Cell Biol. Int. 22, 751–763.
Naus, C.C., Bani-Yaghoub, M., Rushlow, W., Bechberger, J.F., 1999. Consequences of impaired gap junctional communication in glial cells. Adv. Exp. Med. Biol. 468, 373–381.
Ovanesov, M.V., Sauder, C., Rubin, S.A., Richt, J., Nath, A., Carbone, K.M., Pletnikov, M.V., 2006. Activation of microglia by Borna disease virus infection: *in vitro* study. J. Virol. 80, 12141–12148.
Paxinos, G., Watson, C., 1998. The Rat Brain. Academic Press, San Diego.
Pletnikov, M.V., Jones, M.L., Rubin, S.A., Moran, T.H., Carbone, K.M., 2001. Rat model of autism spectrum disorders. Genetic background effects on Borna disease virus-induced developmental brain damage. Ann. N. Y. Acad. Sci. 939, 318–319.
Pletnikov, M.V., Moran, T.H., Carbone, K.M., 2002. Borna disease virus infection of the neonatal rat: developmental brain injury model of autism spectrum disorders. Front. Biosci. 7, d593–d607.
Reuss, B., Dermietzel, R., Unsicker, K., 1998. Fibroblast growth factor 2 (FGF-2) differentially regulates connexin (cx) 43 expression and function in astroglial cells from distinct brain regions. Glia 22, 19–30.
Rozental, R., Campos de Carvalho, A.C., Spray, D.C., 2000. Nervous system diseases involving gap junctions. Brain Res. Brain Res. Rev. 32, 189–191.
Sauder, C., de la Torre, J.C., 1999. Cytokine expression in the rat central nervous system following perinatal Borna disease virus infection. J. Neuroimmunol. 96, 29–45.
Sauder, C., Hallensleben, W., Pagenstecher, A., Schneckenburger, S., Biro, L., Pertlik, D., Hausmann, J., Suter, M., Staeheli, P., 2000. Chemokine gene expression in astrocytes of Borna disease virus-infected rats and mice in the absence of inflammation. J. Virol. 74, 9267–9280.
Scemes, E., Dermietzel, R., Spray, D.C., 1998. Calcium waves between astrocytes from Cx43 knockout mice. Glia 24, 65–73.
Schipke, C.G., Boucsein, C., Ohlemeyer, C., Kirchhoff, F., Kettenmann, H., 2002. Astrocyte Ca^{2+} waves trigger responses in microglial cells in brain slices. FASEB J. 16, 255–257.
Schousboe, A., Waagepetersen, H.S., 2005. Role of astrocytes in glutamate homeostasis: implications for excitotoxicity. Neurotox. Res. 8, 221–225.
Söhl, G., Willecke, K., 2003. An update on connexin genes and their nomenclature in mouse and man. Cell. Commun. Adhes. 10, 173–180.
Söhl, G., Guldenagel, M., Beck, H., Teubner, B., Traub, O., Gutierrez, R., Heinemann, U., Willecke, K., 2000. Expression of connexin genes in hippocampus of kainate-treated and kindled rats under conditions of experimental epilepsy. Brain Res. Mol. Brain Res. 83, 44–51.
Spray, D.C., Duffy, H.S., Scemes, E., 1999. Gap junctions in glia. Types, roles, and plasticity. Adv. Exp. Med. Biol. 468, 339–359.
Stitz, L., Bilzer, T., Planz, O., 2002. The immunopathogenesis of Borna disease virus infection. Front. Biosci. 7, d541–d555.
Stout, C.E., Costantin, J.L., Naus, C.C., Charles, A.C., 2002. Intercellular calcium signaling in astrocytes via ATP release through connexin hemichannels. J. Biol. Chem. 277, 10482–10488.
Tabernero, A., Medina, J.M., Giaume, C., 2006. Glucose metabolism and proliferation in glia: role of astrocytic gap junctions. J. Neurochem. 99, 1049–1061.
Theis, M., Jauch, R., Zhuo, L., Speidel, D., Wallraff, A., Döring, B., Frisch, C., Söhl, G., Teubner, B., Euwens, C., Huston, J., Steinhäuser, C., Messing, A., Heinemann, U., Willecke, K., 2003. Accelerated hippocampal spreading depression and enhanced locomotory activity in mice with astrocyte-directed inactivation of connexin43. J. Neurosci. 23, 766–776.

Ventura, R., Harris, K.M., 1999. Three-dimensional relationships between hippocampal synapses and astrocytes. J. Neurosci. 19, 6897–6906.

Weissenböck, H., Hornig, M., Hickey, W.F., Lipkin, W.I., 2000. Microglial activation and neuronal apoptosis in Bornavirus infected neonatal Lewis rats. Brain Pathol. 10, 260–272.

Welsh, J.P., Yuen, G., Placantonakis, D.G., Vu, T.Q., Haiss, F., O'Hearn, E., Molliver, M.E., Aicher, S.A., 2002. Why do Purkinje cells die so easily after global brain ischemia? Aldolase C, EAAT4, and the cerebellar contribution to posthypoxic myoclonus. Adv. Neurol. 89, 331–359.

Yamaoka, Y., Shimohama, S., Kimura, J., Fukunaga, R., Taniguchi, T., 1993. Neuronal damage in the rat hippocampus induced by *in vivo* hypoxia. Exp. Toxicol. Pathol. 45, 205–209.

Ye, Z.C., Wyeth, M.S., Baltan-Tekkok, S., Ransom, B.R., 2003. Functional hemichannels in astrocytes: a novel mechanism of glutamate release. J. Neurosci. 23, 3588–3596.

Zocher, M., Czub, S., Schulte-Mönting, J., de La Torre, J.C., Sauder, C., 2000. Alterations in neurotrophin and neurotrophin receptor gene expression patterns in the rat central nervous system following perinatal Borna disease virus infection. J. Neurovirol. 6, 462–477.